University of Leipzig
Faculty of Physics and Earth Sciences
Advanced practical course in physics

Protocol

Optical spectroscopy of color centers and molecules

Submitted by: xxx
Pascal Schumann

Supervisor: M. Sc. Dominic Reinhardt
Faculty of Physics and Earth Sciences

Experiment: 07.11.2023

Delivery: 02.12.2023

Table of contents

1 Theoretical considerations

1.1 Molecular spectra

1.1.1 Electronic transitions

The electronic transitions in molecules are realized by raising electrons to higher energy states. In multi-electron systems, only the electrons on the non-closed shells are considered, as their orbital angular momentum does not cancel out as in the case of the closed shells. The orbital angular momentum of the corresponding electrons on the unsealed shells is therefore added to the total orbital angular momentum of the electron shell, which assumes integer multiples of $\hbar$, which are then named with the Greek letters Σ, Π, Δ, Φ instead of numbers. According to quantum mechanics, the selection rule applies to electronic transitions

$$\Delta\Lambda = 0, \pm 1. \tag{1.1}$$

The same applies to the total spin S, as this is also made up of the spins of the electrons on the shells that are not fully occupied. Since spin and orbital angular momentum interact with each other, the energy levels from the orbital angular momentum split into $2S + 1$ values each, which is also referred to as multiplicity M. If we now consider diatomic molecules, the symmetry must also be taken into account, in contrast to the atom. Therefore, it is also necessary to know whether a state function inverted at the center of symmetry is symmetrical or antisymmetrical to its initial form. If a phase jump occurs at the boundary, the function is described as odd
"u", if this is not the case, as an even "g". In addition, a mirror-symmetric function is characterized with a "+" and the antisymmetric variant with a "-". This results in the following form for the complete description of the electron state of a molecule

$$^{M}\Lambda^{\pm}_{(g,u)}. \tag{1.2}$$

1.1.2 Molecular vibrations

In addition, the interactions between the atoms of the molecule must be considered.

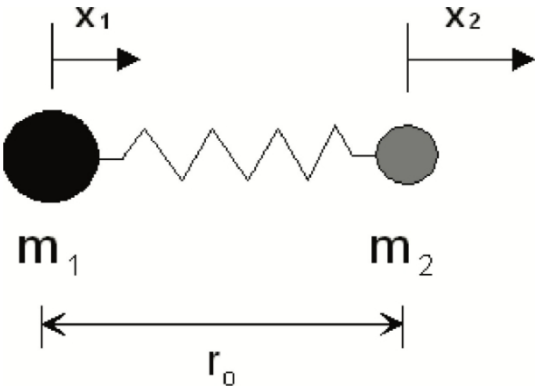

Figure 1.1: Diatomic molecule as a harmonic oscillator (Riede(n.d.))

For this purpose, the harmonic oscillator model is used and the equations of motion for a diatomic molecule are obtained by considering the forces

$$m_1 \ddot{x}_1 = -k(x_1 - x)_2 \quad (1.3)$$

$$m_2 \ddot{x}_2 = -k(x_2 - x_1), \quad (1.4)$$

which can be converted via
$x = x_1 - x_2$ to

$$\ddot{x} = -\frac{k}{\mu}x \quad (1.5)$$

can be summarized. The resonance wave number of such a harmonic oscillator is then

$$\bar{\nu}_s = \frac{1}{2\pi c}\sqrt{\frac{k}{\mu}}. \quad (1.6)$$

To calculate the energy values, solve the Schrödinger equation for the potential

$$U = 2\pi c^{22} y^{-2} \mu x^2, \quad (1.7)$$

which is derived from the back-driving force via

$$\frac{dU}{dx} = -F = -kx \tag{1.8}$$

with the approach

$$x = x_0 \sin(2\pi c \bar{\nu}_s t) \tag{1.9}$$

is obtained. This also provides discrete energy levels

$$E(n) = hc\bar{\nu}_s \left(n + \frac{1}{2}\right); n \in \mathbb{N}_0, \tag{1.10}$$

with the selection rule

$$\Delta n = \pm 1. \tag{1.11}$$

Experimentally, however, there are no constant distances between the vibrational energies, but these become smaller at higher n and, in addition, it is known that the molecule must dissociate at a sufficiently large distance. In addition, the strong nuclear force must be taken into account at small distances. Therefore, a transition from the model of the harmonic oscillator to the Morse potential is recommended.

$$U = E_D a^2 x^2 \tag{1.12}$$

for which the approximation of the harmonic oscillator is only given for small x, where E_D represents the dissociation energy and

$$a = 2\pi\bar{\nu}_s c \sqrt{\frac{\mu}{2E_D}} = \omega_s \sqrt{\frac{\mu}{E_D}} \tag{1.13}$$

is a characteristic constant of the molecule. Solving the Schrödinger equation with this potential leads to the approximated energy eigenvalues

$$E(n) = hc\bar{\nu}_s \left(n + \frac{1}{2}\right) - \gamma_e \left(n + \frac{1}{2}\right)^2, \tag{1.14}$$

where γ_e is the anharmonicity constant. This results in the following diagram for the anharmonic oscillator.

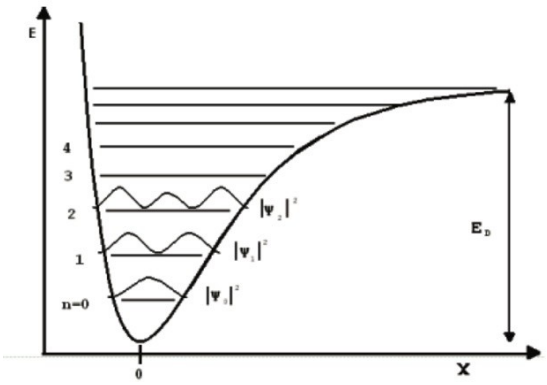

Figure 1.2: Energy eigenvalues of the anharmonic oscillator (Riede (n.d.))

1.1.3 Combined transitions

If you now want to combine the findings of the two isolated observations for electrical and oscillation transitions, you also have to consider the alternating effect. The respective equilibrium distance for the vibrations depends on the electronic state, which can have various consequences. Either the binding energy remains the same in relation to the distance (a), it becomes larger (b) or smaller (c) in the excited state. The Franck-Condon principle also applies here, i.e. the electronic transitions take place significantly faster than the vibration of the molecules, which is why the transitions in the diagram are vertical.

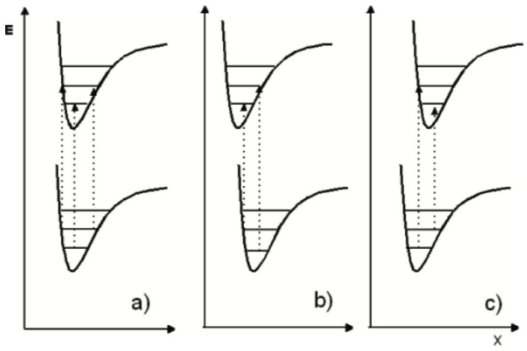

Figure 1.3: Electronic transitions with altered equilibrium distances (Riede (n.d.))

For the transition energy between two levels n' and n'' this results in

$$\Delta E(n', n'') = E(n') - E(n'') = E_{elektr} + hc\bar{\nu}_s \left(n' + \frac{1}{2}\right) - hc\bar{\nu}_s \left(n'' + \frac{1}{2}\right) \quad (1.15)$$
$$- hc\bar{\nu}_s \gamma_e \left(n' + \frac{1}{2}\right)^2 + hc\bar{\nu}_s \gamma_e \left(n'' + \frac{1}{2}\right)^2 .$$

To dissociate the molecule, however, it is not sufficient to supply it with the energy E_D , as the transitions for large Δn are very unlikely.

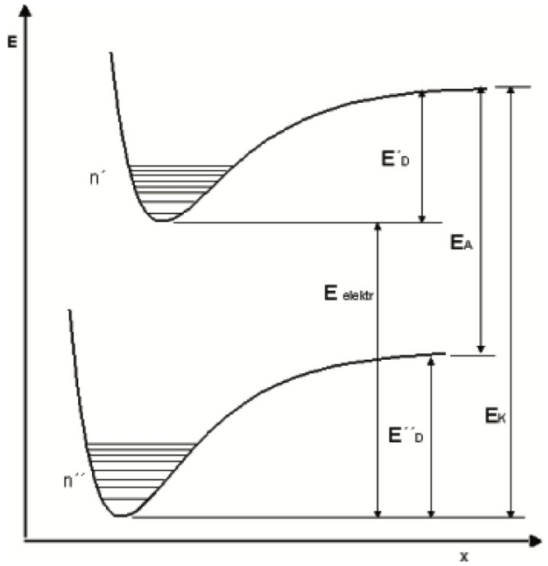

Figure 1.4: Definition of the individual energies (Riede (undated))

However, if an electron is excited, the transition probability increases and the transition energy between states with n' and n'' results in

$$\Delta E = E_{Electric} + E_S \left(n' + \frac{1}{2}\right) - E_S \gamma_e \left(n + \frac{1}{2}\right)^2 . \quad (1.16)$$

For high n' the values converge towards E_K and two lines with a quantum difference of N differ by

$$\Delta(\Delta E) = E_S'\left(n' + N + \frac{1}{2}\right) - E_S'\left(n' + \frac{1}{2}\right) - E_S'\gamma_e'\left(n' + N + \frac{1}{2}\right)^2 + E_S'\gamma_e'\left(n' + \frac{1}{2}\right)^2$$
$$= E_S'N - E_S'\gamma_e'N(2n' + N + 1) \quad (1.17)$$

resp.

$$\Delta(\Delta E) = E_S'(1 - \gamma_e'(n' + 1)) \quad (1.18)$$

for $N = 1$, where the distance between two neighboring line spacings depends linearly on n'
and therefore

$$\Delta(\Delta E)(n') - \Delta(\Delta E)(n' + 1) = -2E_S'\gamma_e' = \text{const.} \quad (1.19)$$

applies. As this distance disappears for $E = E_K$, the following also results

$$n_e' = \frac{1}{2\gamma_e'} - 1 \quad (1.20)$$

which can now be used to calculate n' .

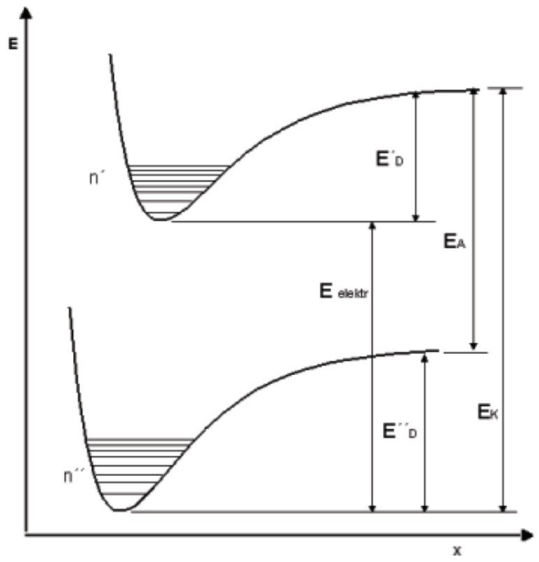

Figure 1.5: Definition of energies (Riede (n.d.))

If in equation (1.16) $n = n'$ $_e$ you get

$$\Delta E(n = n'_e) = E_{\text{Electric}} + E'_S n'_e + \frac{1}{2} E_S \gamma'_e n'^2_e \qquad (1.21)$$

This can be used to calculate E_{elektr}, whereby E_A and E'_S are assumed to be known. can be set. The following applies: $E'_S = 0.0159$ eV and $E_A = 0.94$ eV

1.2 Color centers

Color centers are ionic defects in the lattice of alkali halogens that are occupied by electrons. They are created by chemical processes or high-energy radiation (e.g. X-rays). These electrons are then no longer strongly localized, as is normally the case. However, this does not apply to the electronic states of the color centers, which are located in the otherwise very large band gap of a crystal without defects. For aluminum halides, the energy of such electronic states is in the visible spectral range. This is how color centers get their name.

1.2.1 Classic description

Due to the lack of negative charge of the anion at the defect site, the excess positive charge of the surrounding ions is assigned to the volume of the defect site, which is described as a sphere with radius R. The following applies

$$R = \sqrt[3]{\frac{3\sqrt{2}}{16\pi}}\, a^3. \qquad (1.22)$$

A homogeneous charge density is now assumed in this volume, which acts on the electron at the location with a radial electric field. Since the total charge in the volume must be just one positive elementary charge, the following results via

$$e^+ = \int \rho dV = \rho \frac{4\pi}{3} R^3 \qquad (1.23)$$

and Maxwell's equation

$$divD = \rho \tag{1.24}$$

the electric field to

$$E_r = \frac{\rho r}{3\varepsilon\varepsilon_0} = -\frac{e\, r^+}{4\pi\varepsilon\varepsilon_0 R^3}. \tag{1.25}$$

This gives the Coulomb force and thus also the equation of motion

$$F_r = mr^{\cdot\cdot} = e\, E_r = \frac{-e\, r^2}{4\pi\varepsilon\varepsilon_0 R^3} \tag{1.26}$$

and by transforming it into an oscillation equation also the angular frequency

$$\omega = \frac{e^2}{4\pi\varepsilon\varepsilon_0 m R^3}. \tag{1.27}$$

Finally, the excitation energy with

$$E = \hbar\omega = \frac{he}{\pi\sqrt{(3\ 2m\varepsilon\varepsilon_0\ a^3)^{\frac{1}{2}}}}. \tag{1.28}$$

1.2.2 Quantum mechanical description

For the quantum mechanical consideration of color centers, a three-dimensional box potential with edge lengths a, b and c and infinitely high walls is assumed. Within this box, the following results

$$-\frac{\hbar}{2m}\Delta\Psi = E\Psi \tag{1.29}$$

resp.

$$\Delta\Psi = -\alpha\Psi \tag{1.30}$$

with

$$\alpha = \frac{2mE}{\hbar^2}. \tag{1.31}$$

Since the Laplace operator is a sum of twofold derivatives in the three spatial directions, the product function

$$\Psi = \Psi_1(x)\Psi_2(y)\Psi_3(z) \tag{1.32}$$

to . Applying the Laplace operator then results in

$$_1\Delta\Psi(x)\Psi_2(y)\Psi_3(z) = -\alpha\Psi_1(x)\Psi_2(y)\Psi_3(z)\,. \tag{1.33}$$

If we now divide by the product function, we arrive at

$$\frac{1}{{}_3\Psi(z)}\frac{\partial^2\Psi_3(z)}{\partial z^2} + \frac{1}{\Psi(y)}\frac{\partial^2\Psi_2(y)}{\partial y^2}\,{}_2 + \frac{1}{\Psi(x)}\frac{\partial^2\Psi_1(x)}{\partial x^2}\,{}_1 = -\alpha. \tag{1.34}$$

With x, y and z as independent variables and the constant α, the individual summands must also be constants, which are now written as

$$\frac{1}{{}_1\Psi(x)}\frac{\partial^2\Psi_1(x)}{\partial x^2} = -\alpha_1 \tag{1.35}$$

$$\frac{1}{\Psi_2(y)}\frac{\partial^2\Psi_2(y)}{\partial y^2}\,{}_1 = -\alpha_2 \tag{1.36}$$

$$\frac{1}{\Psi_3(z)}\frac{\partial^2\Psi_3(z)}{\partial z^2} = -\alpha_3 \tag{1.37}$$

wit
h

$$\alpha = \alpha_1 + \alpha_2 + \alpha_3\,, \tag{1.38}$$

which decouples the coordinates. This allows the differential equations to be solved separately using the harmonic approach

$$_1\Psi(x) = A_1\sin(\beta_1 x) \tag{1.39}$$

$$_2\Psi(y) = A_2\sin(\beta_2 y) \tag{1.40}$$

$$_3\Psi(z) = A_3\sin(\beta_3 z) \tag{1.41}$$

and the still unknown constants A and β_i . By inserting the wave functions one

obtains

$$\beta_i^2 = \alpha_i \,,\; i = 1,\, 2,\, 3 \,, \tag{1.42}$$

which is why only the boundary conditions need to be fulfilled in order to determine A. Due to the box potential, these are $\Psi_1\,(x = 0) = \Psi_1\,(x = a) = 0$ (analogous for the other two directions). While the first case is automatically fulfilled with the sine function, the second condition yields

$$\beta_1 = \frac{n_1 \pi}{a} \,,\; n_1 = 1,\, 2,\, 3,\, \ldots \tag{1.43}$$

$$\beta_2 = \frac{n_2 \pi}{b} \,,\; n_2 = 1,\, 2,\, 3,\, \ldots \tag{1.44}$$

$$\beta_3 = \frac{n_3 \pi}{c} \,,\; n_3 = 1,\, 2,\, 3,\, \ldots \,, \tag{1.45}$$

with which the energy eigenvalues

$$E = \frac{\hbar^2 \pi^2}{2m} \left(\frac{n_1^2}{a^2} + \frac{n_2^2}{b^2} + \frac{n_3^2}{c^2} \right) \tag{1.46}$$

is obtained. Finally, to obtain the constants A_i , use the normalization

$$\int_0^a \int_0^b \int_0^c |\Psi(x, y, z)|^2 \, \mathrm{d}x\mathrm{d}y\mathrm{d}z = 1 \tag{1.47}$$

and thus arrives at the final wave function

$$\Psi = \Psi_{n_1, n_2, n_3} = \sqrt{\frac{8}{abc}} \sin\left(\frac{n_1 \pi x}{a}\right) \sin\left(\frac{n_2 \pi y}{b}\right) \sin\left(\frac{n_3 \pi z}{c}\right) \,, \tag{1.48}$$

which with the associated energy

$$E_{n_1, n_2, n_3} = E_0 \left(n_1^2 + n_2^2 + n_3^2 \right) \,,\; E_0 = \frac{\pi^2 \hbar^2}{2ma^2} \tag{1.49}$$

agrees well with the experimental results. For the transition from the ground state to the first excited state, the following results are obtained

$$E_m = \frac{3h^2}{8ma^2} \,. \tag{1.50}$$

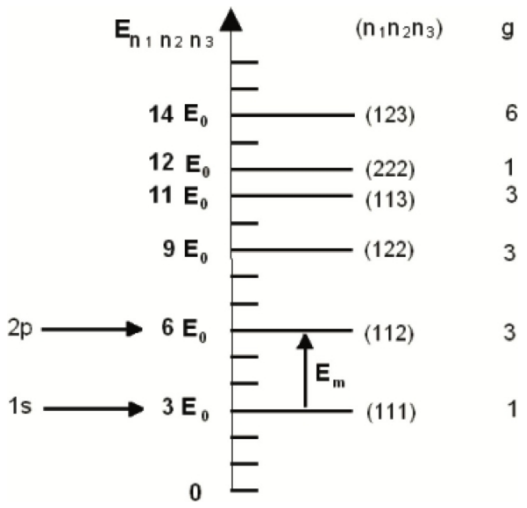

Figure 1.6: Energies in the three-dimensional box potential (Riede (n.d.))

1.2.3 Line width

Although one would theoretically expect very narrow absorption bands due to the discrete energy levels, these are relatively broad. The background is the interaction of the electron with the surrounding lattice vibrations, which is why the configuration coordinate R is introduced, which describes the distance of the surrounding cations from the center of the color center. In the excited states, the electron takes up more space, which results in R being minimal for the 1s state. The parabolas of the energy shift with the different values of R and the various excited states of the electron, which together with the Franck-Condon principle, which explains the vertical transitions, leads to relatively broad emission and absorption bands.

1.2.4 Determining the concentration of color centers

To determine the concentration N of the color centers in the examined lattice, integral absorption is used due to its proportionality. With the approximation by a Lorentz curve and the Drude dispersion theory, the integral absorption results in

$$\int_{nm} \alpha d\nu = \frac{e^2 N}{4c2\epsilon_0} \frac{A}{3} \left(\frac{n^2 + 2}{3} \right)^{B_2} \tag{1.51}$$

1
2

with the refractive index n and the mass m of the electron. The absorption coefficient is obtained via the transmission, i.e. the ratio of the intensities in front of and behind the sample with

$$T = \frac{I_t}{I_0} = \frac{(1 - R)\, e^{2-\alpha d}}{1 - R^2 e^{-2\alpha d}} \tag{1.52}$$

and

$$R = \frac{(n - 1)^2}{(n + 1)^2}. \tag{1.53}$$

If R "1 you get Lambert-Beer's law

$$I = I_0 e^{-\alpha d}. \tag{1.54}$$

2 Experimental setup

The *Lambda 365* spectrometer used is a dual-beam spectrometer with the following beam path.

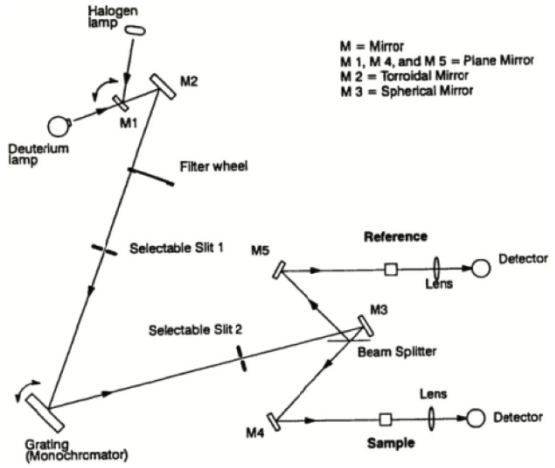

Figure 2.1: Beam path of the spectrometer (Riede (n.d.))

The wavelength range of the spectrometer extends from 1100 nm to 200 nm. This is achieved using two different lamps, which are switched between at 400 nm. A beam splitter splits the light into a measurement beam and a reference beam, so that it is possible to immediately record a transmission spectrum without the need for a reference measurement. A reflection grating makes it possible to set the wavelength that hits the sample very precisely. By rotating this grating, the entire wavelength range can be traversed.
The resolution of the spectrum can be influenced using two settings: Firstly, the slit width can be set via a selectable slit. Secondly, it is possible to set how quickly the wavelength range is traversed - the so-called registration speed.
After inserting a sample into the spectrometer, the measurement is started electronically and the transmission spectrum is immediately displayed in the associated software.

3 Task definition

Task 1

The wavelength accuracy of the *Lambda 365* spectrometer is to be checked using the absorption bands of the holmium oxide filter. The influence of the slit width and the registration speed on the spectrum must be investigated.

Task 2

The transmission spectra of a glass and quartz glass cuvette filled with air and water are to be recorded and interpreted. Furthermore, depending on the angle of incidence, the transmission spectrum of an interference filter is to be recorded and discussed. In addition, the spectral range to which the eye is sensitive is to be determined. Furthermore, transmission curves of color filters can be recorded.

Task 3

The transmission spectrum of iodine vapor is to be measured and the convergence energy, the dissociation energy in the ground and excited state and the energy of the electronic transition are to be determined.

Task 4

F centers are to be generated in a KBr crystal by UV irradiation and their transmission spectra measured. The concentration of these centers as a function of the time after irradiation is to be determined from the integral absorption. The excitation energy and the line width must be determined.

Task 5

The transmission spectrum is to be recorded for a NaCl crystal in which F centers have been generated with X-rays. The excitation energy, the line width and the concentration of the centers are to be determined.

Task 6

The excitation energy of the F centers in KBr and NaCl is to be calculated using a classical and a quantum mechanical model and compared with the experimental values. The results of both models are to be discussed. Using the quantum mechanical model, determine the lattice constant from the measured excitation energy.

4 Evaluation of task 1

4.1 Calibration

For the measurement of the holmium oxide filter, the spectrum was displayed and then the minima given from the test documents were entered and compared with those actually measured. This comparison allows conclusions to be drawn about the calibration of the device. Only the wavelengths in the relevant range (presence of calibration bands) are shown in the graph.

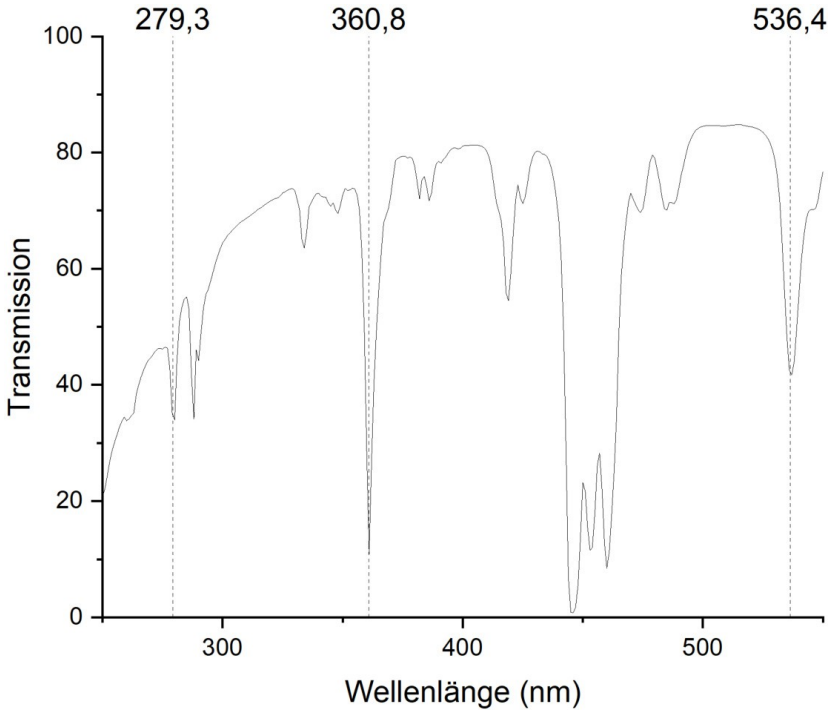

Figure 4.1: Spectrum of the holmium oxide filter with calibration bands

It can be seen that the deviation is very small. The device only outputs measured values for the settings made for integer shaft lengths, which is why the minima never lie directly on the calibration band. It appears,

as if the measured values were systematically too large - however, with three comparison values, this can also be explained by random measurement errors. For further considerations, an inaccuracy of the measured wavelength of $u(\lambda) = \pm 1$ nm is assumed.

4.2 Recording speed

The speed at which the measurement is taken can be set.
This registration speed is specified in $\frac{\text{nm}}{\text{min}}$. To determine the effects
In order to observe a change in this parameter, measurements of the spectrum of the holmium oxide filter were recorded at three different registration speeds. The slit width was left constant at 0.5 nm.

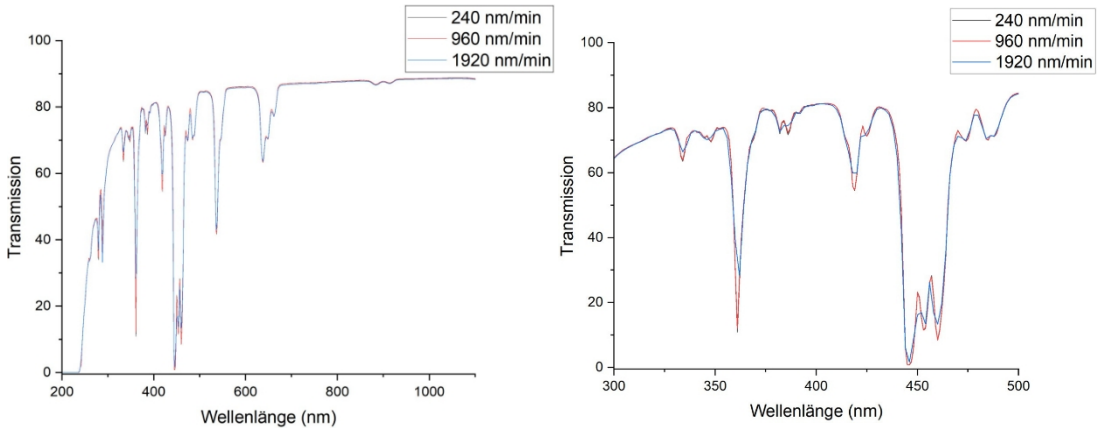

(a) Recorded spectra **(b)** Enlarged section

Figure 4.2: Influence of the recording speed

It can be seen that the amplitude of the minima decreases as the registration speed increases. It is particularly noticeable in the enlarged section that some double bands can no longer be perceived as such at higher registration speeds. In the worst case, a minimum can no longer be detected at all. A higher registration speed therefore results in a reduction in resolution.

4.3 Gap width

The device has a setting for the width of the slit through which the light shines on the sample. In order to investigate the effects of changing this parameter, measurements were taken with three different slit widths, while the registration speed was kept constant at 240 $\frac{nm}{min}$ was left in place.

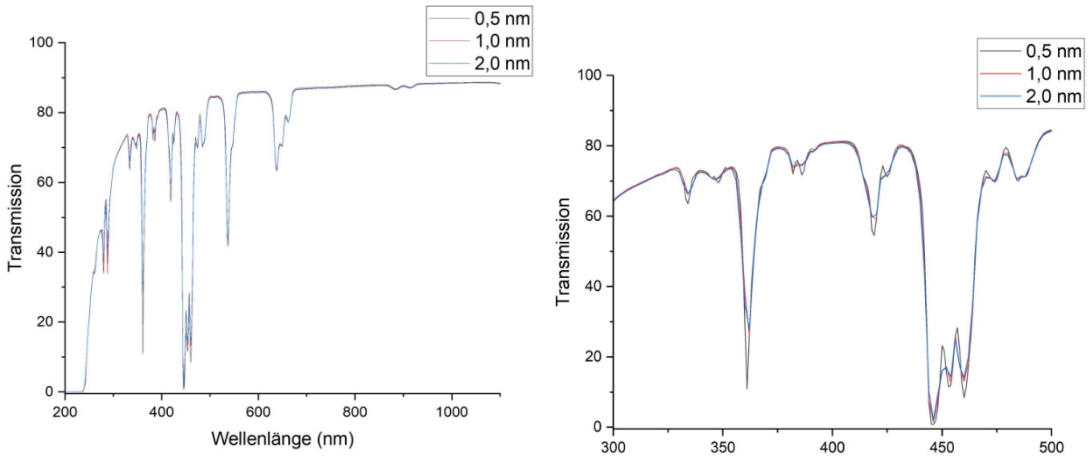

(a) Recorded spectra **(b)** Enlarged section

Figure 4.3: Influence of the gap width

The amplitudes of the minima decrease with increasing slit width, while their half-widths increase slightly. In turn, it is sometimes difficult to precisely identify a minimum at higher slit widths. In some cases, the positions of the minima shift significantly compared to the higher slit width. Double bands can generally no longer be clearly identified at higher slit widths. A higher slit width therefore results in a reduction in resolution.

Unless otherwise specified, all further measurements are taken at a gap width of 0.5 nm and a registration speed of 480 $\frac{nm}{min}$. leads.

5 Evaluation of task 2

5.1 Cuvettes

The spectrum was recorded for a glass or quartz glass cuvette - filled with air or water respectively.

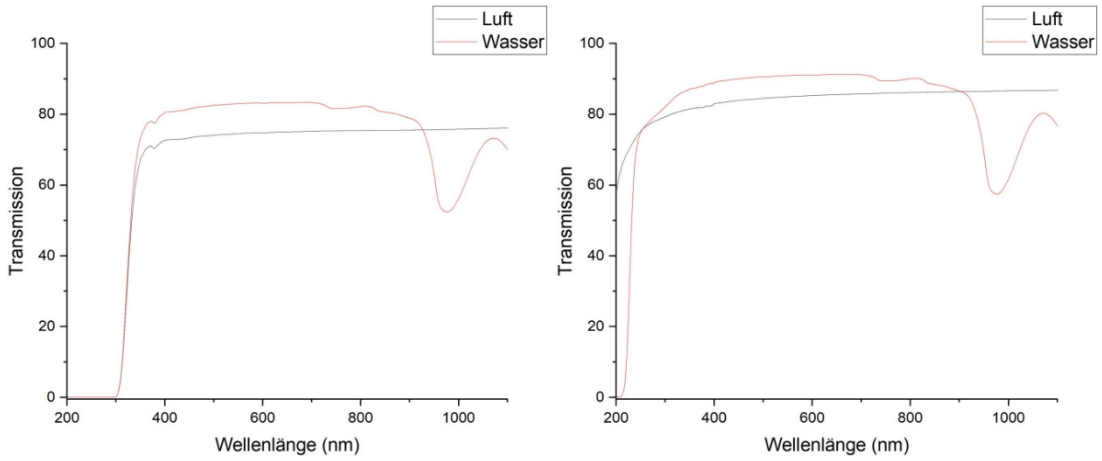

(a) Glass cuvette **(b)** Quartz glass cuvette

Figure 5.1: Spectra of the cuvettes

It can be seen that the range in which the glass blocks is significantly larger than that of quartz glass. Glass blocks below about 300 nm. No statement can be made for quartz glass. An extended minimum can be seen in the cuvettes filled with water. These wavelengths are absorbed to a small extent by water. It is noticeable that the transmission of cuvettes filled with water is generally somewhat higher. This can be explained with the help of the refractive indices. The refractive index of water is around 1.3 to 1.5 in the wavelength range under consideration; that of glass or quartz glass is around 1.5. Consequently, the difference between the refractive indices is significantly lower for the cells filled with water than for those filled with air ($n \approx 1$). This has a corresponding effect on the transmittance and reflectance, as can be seen above.

5.2 Interference filter

An interference filter was used at different angles to the incoming beam and the spectrum was measured in each case.

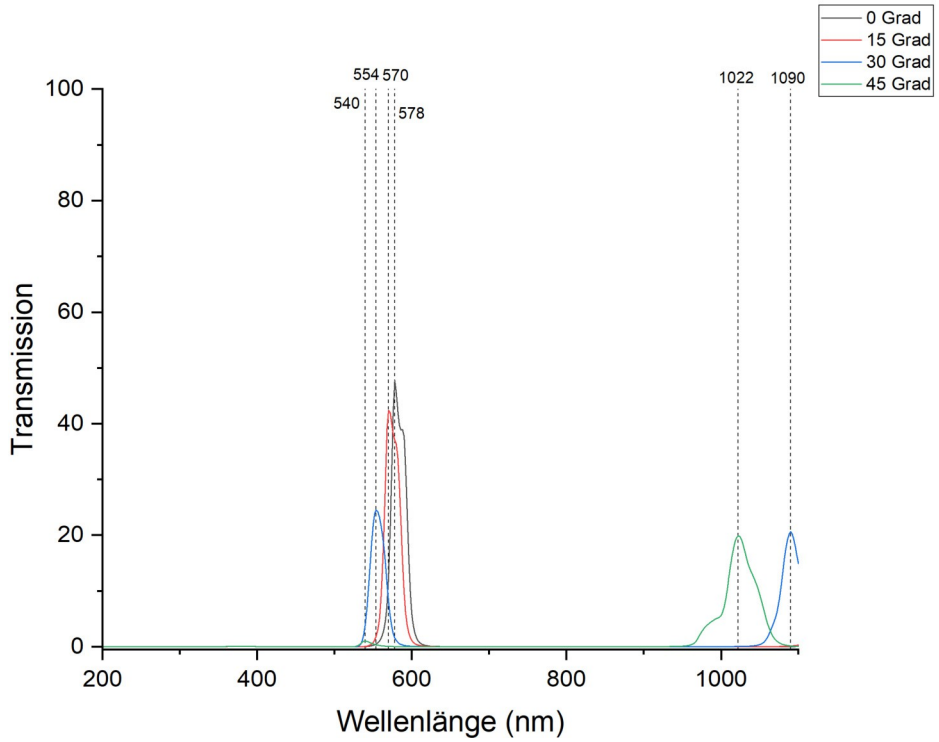

Figure 5.2: Spectrum of the interference filter at different angles

The transmission maxima were marked in each case. The interference filter only transmits a certain small wavelength range. All other wavelengths are reflected or interfere destructively, so that the interference filter has a broad blocking range. Changing the angle in relation to the measurement beam changes the effective layer thickness of the filter, which changes the interference behavior, i.e. another wavelength interferes constructively (and is therefore transmitted). The fact that these are interference phenomena can be seen, for example, in the 30-degree spectrum, in which one maximum is approximately twice the wavelength of the other.

5.3 Color filter

The spectrum of various color filters was recorded. The visible light range from around 400 nm to 800 nm is particularly relevant.

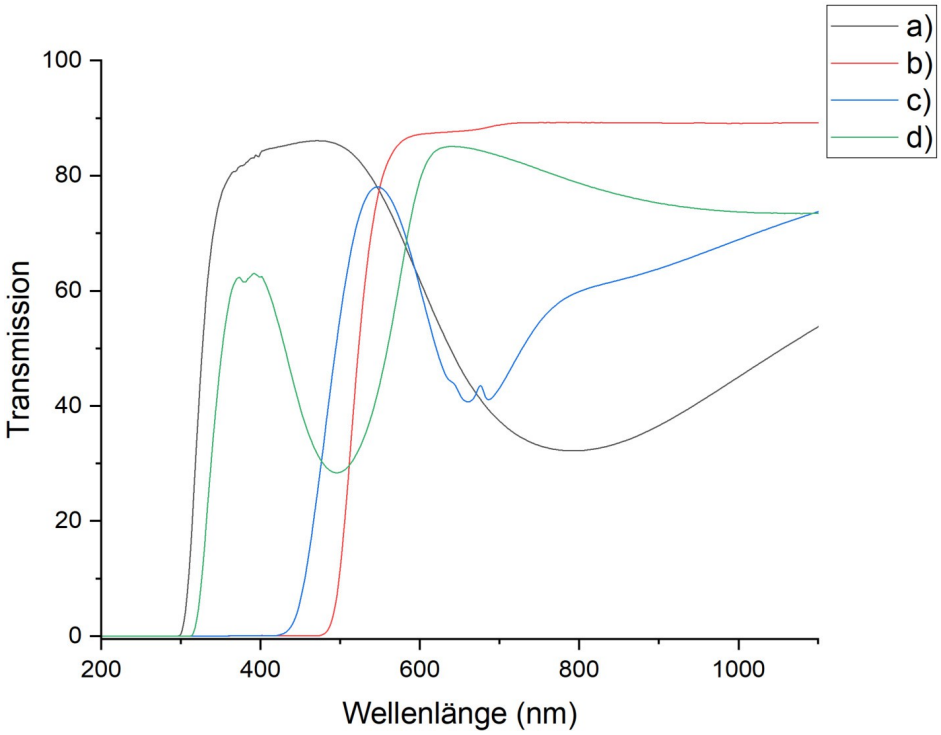

Figure 5.3: Spectrum of the different color filters

Color filter a) transmits particularly in the blue light range, but also has significant amounts in the remaining visible range. It is therefore a filter that should appear light blue.
Color filter b) transmits in the yellow to red range. As the eye is somewhat more sensitive to yellow, yellow should also be more prominent.
Color filter c) has the maximum transmission in the range of green to yellow light, so should have a mixture of these two colors.
Color filter d) has its maximum in the red light range and should therefore also take on this color.

6 Evaluation of task 3

The spectrum of iodine vapor was measured with a slit width of 0.5 nm and a recording speed of $120\frac{nm}{min}$ in order to achieve a particularly high recording speed. resolution.

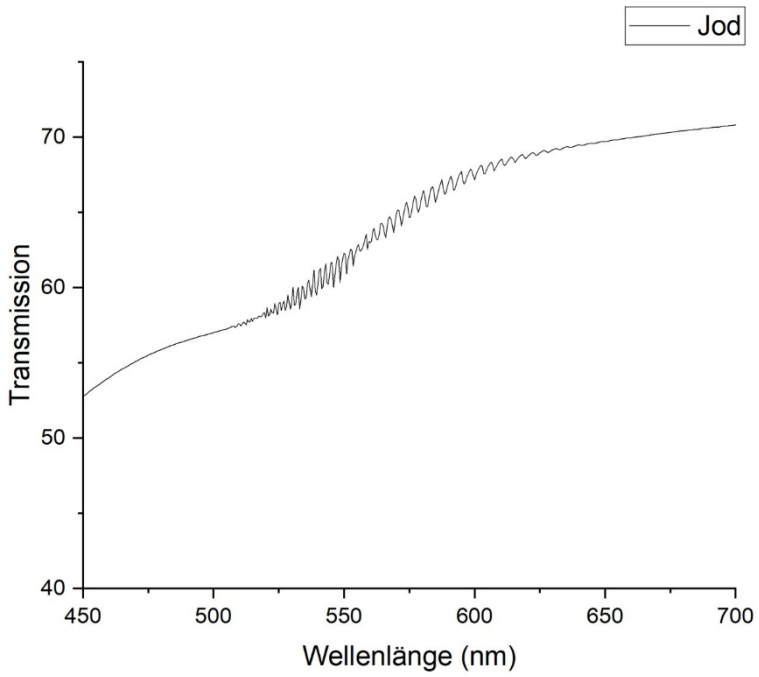

Figure 6.1: Spectrum of iodine vapor

The wavelengths of the minima were read off and converted into energies (eV). According to equation (1.18), their differences must be linear. A corresponding fit provides the increase.

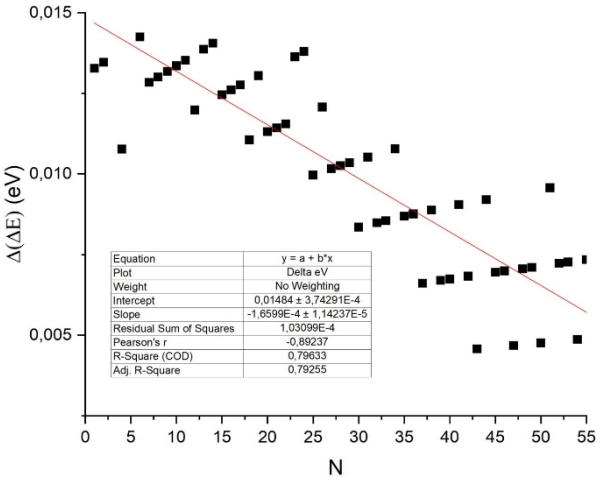

Figure 6.2: Linear fit of the energy differences

The anharmonicity constant y_e = (5.22 0.36) 10^{-3} follows from the above equation and the increase. Equation (1.20) immediately gives n_E = 94.79 6.61. The condensation energy can now be calculated. Because of
$\Delta(\Delta E)) = 0$ for E_K you only need to find the energy of the correspondingly assigned N. With the above relationship, this corresponds to the triangular area between the graph, the *x-axis* and the *y-axis*, to which the energy of the first transition (N = 1) is added. The result is E_K = (2.55 ± 0.08) eV. Equation (1.21) now gives $_{\text{Eelektr}}$ = (1.79 ± 0.14) eV. The dissociation energies are now obtained using figure (1.5) by E_D'' = (1.61 ± 0.08) and E_D' = (0.76 ± 0.22) eV.

7 Evaluation of task 4

A spectrum of the KBr crystal was recorded immediately after irradiation with UV light and 10 min, 20 min and 40 min afterwards. In addition, a reference was recorded for the non-irradiated crystal.

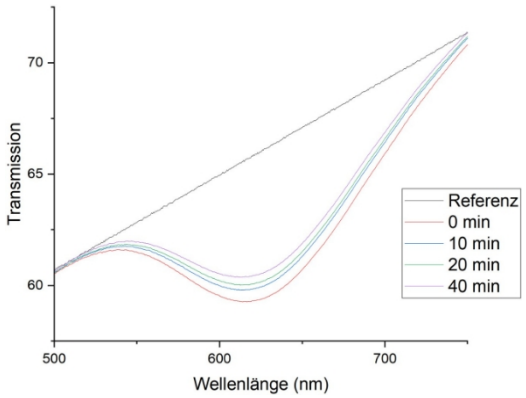

Figure 7.1: Spectra of the KBr crystal

The deviation of the spectra from the reference was shown for the various points in time.

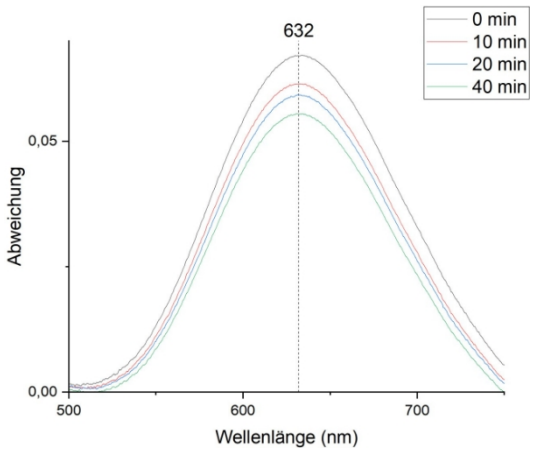

Figure 7.2: Deviation from the reference spectrum

The maximum was entered. It corresponds to the excitation energy of E_A = (1.961 0.004± eV. If the deviation is plotted against the wavenumber, the integral absorption can be calculated. The concentration of F centers in the crystal follows from this using equation (1.51). One finds

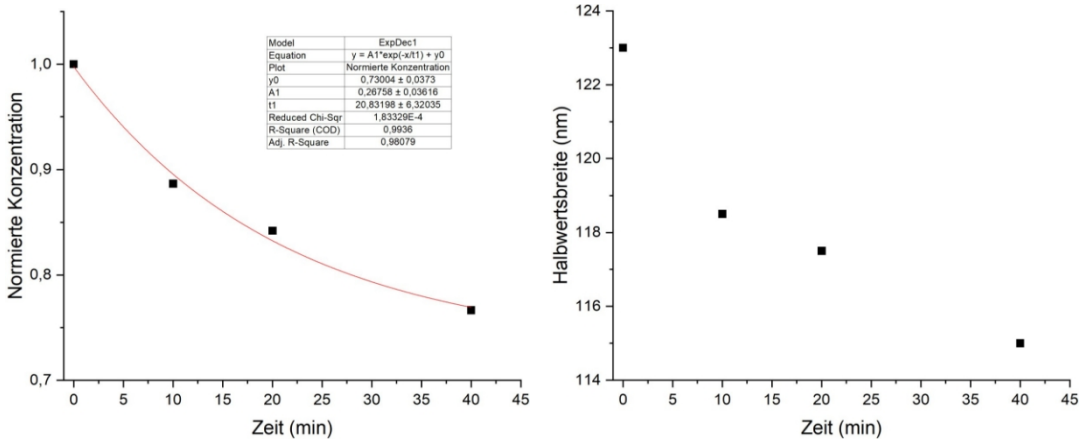

(a) Concentration normalized to initial concentration

(b) Half-width of the bands

Figure 7.3: Concentration and line width

and thus, as expected, an exponential decrease over time. N_0 = 1, 790 10 m^{18} $^{-3}$. The half-widths of the absorption bands are shown on the right.

8 Evaluation of task 5

A reference spectrum and a spectrum after irradiation with X-rays were recorded from the NaCl crystal.

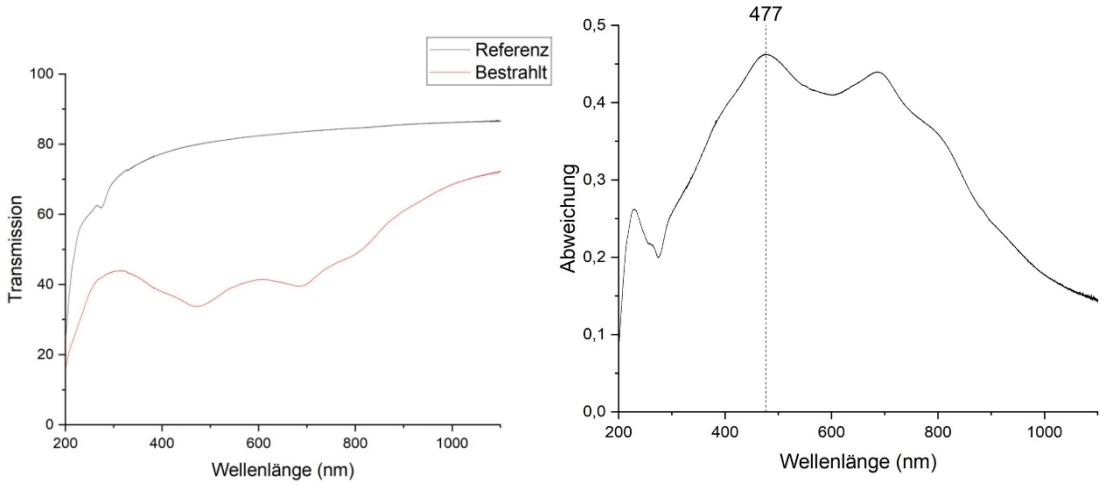

(a) Spectra **(b)** Deviation

Figure 8.1: NaCl crystal

It is difficult to see where the color centers had an influence. The peak with the highest amplitude is marked, which corresponds to an excitation energy of E_A = (2.600 0.006) eV±Assuming that the additional absorption is only caused by F centers in the NaCl crystal, the concentration of these is N_0 = 1, 051 - 10 m^{20} $^{-3}$.

9 Evaluation of task 6

Equations (1.28) and (1.50) give the following values for the excitation energy

	KBr	NaCl
Classic	0,901	1,111
Quantum mechanical	2,598	3,559
Measured value	1,961	2,600

Table 9.1: Excitation energies in eV

The classical model gives inaccurate predictions. This is due to the assumptions, e.g. a homogeneous charge distribution of the sphere or the possibility of localizing the electron. Influences of the other atoms (apart from the direct neighbors) are also neglected. The assumption of a box potential in the quantum mechanical model, which amounts to a proportionality $E_q \; a^{-2}$, already corresponds quite well with ex- perimental findings in which $E_q \; a^{-1,84}$ was found. The model can be improved by also taking into account the interactions of the electron with surrounding particles.
If the lattice constant is determined from the measured excitation energy using the quantum mechanical model, the result is

$$E_{\mathrm{A,KBr}} = (7,585 \pm 0,008)\mathring{\mathrm{A}}$$
$$E_{\mathrm{A,NaCl}} = (6,587 \pm 0,008)\mathring{\mathrm{A}},$$

in good approximation to the actual values.

10 Bibliography

W. Finkelnburg (1962). Introduction to atomic physics. Springer Verlag (Berlin).
M. Hollas, Modern Spectrosocopy. John Wiley and Sons (Chichester 1992).
M. F. Manfred Böhm (1992). Higher Experimental Physics. Publisher VCH (Weinheim).
Y. Farge and M. P. Fontana (1979). Electronic and Vibrational Properties of Point Defects in Ionic Crystals. Defects in Crystalline Solids 11.
J. J. Markham (1996). F-Centres in Alkali Halides. Solid State Physics Suppl. 8. Bergmann-Schaefer (1992). Textbook of Experimental Physics. de Gruyter (Berlin).
Dr. V. Riede (n.d.). Optical spectroscopy of color centers and molecules (Franck-Condon principle). University of Leipzig.